
UNCERTAINTY HERDING: ONE ACTIVE LEARNING METHOD FOR ALL LABEL BUDGETS

Wonho Bae

University of British Columbia & Borealis AI
whbae@cs.ubc.ca

Gabriel L. Oliveira*

Borealis AI
gabriel.oliveira@borealisai.com

Danica J. Sutherland*

University of British Columbia & Amii
dsuth@cs.ubc.ca

ABSTRACT

Most active learning research has focused on methods which perform well when many labels are available, but can be dramatically worse than random selection when label budgets are small. Other methods have focused on the low-budget regime, but do poorly as label budgets increase. As the line between “low” and “high” budgets varies by problem, this is a serious issue in practice. We propose *uncertainty coverage*, an objective which generalizes a variety of low- and high-budget objectives, as well as natural, hyperparameter-light methods to smoothly interpolate between low- and high-budget regimes. We call greedy optimization of the estimate Uncertainty Herding; this simple method is computationally fast, and we prove that it nearly optimizes the distribution-level coverage. In experimental validation across a variety of active learning tasks, our proposal matches or beats state-of-the-art performance in essentially all cases; it is the only method of which we are aware that reliably works well in both low- and high-budget settings.

1 INTRODUCTION

In active learning, rather than being provided a dataset of input-output pairs as in passive learning, a model strategically requests annotations for specific unlabeled inputs. The aim is to learn a good model while minimizing the number of required output annotations. This procedure is generally iterative: a model is initially trained on a small, labeled dataset, then selects the most “informative” data points from an unlabeled pool to annotate. This is particularly useful when labeling is expensive or time-consuming. For example, manual annotations of medical imaging by radiologists or pathologists may be especially time-consuming and costly. Measuring whether a compound interacts with a certain biological compound may require slow, high-accuracy chemical simulations or even lab experiments. Discovering a customer’s product preferences may require giving them many offers, which is slow, potentially expensive, and may produce a poor customer experience.

The most popular line of work in active learning has used notions of uncertainty to measure how informative each candidate data point is expected to be, and selects data points for labeling to maximize that measure. Although these uncertainty-based approaches often work well in the experimental settings where they are evaluated, Hachohen et al. (2022) and Yehuda et al. (2022) have shown that when there are few total labeled data points – called the *low-budget* setting – they can be substantially worse than random selection, presumably because the model’s estimate of uncertainty is not yet reliable. To address this, they (and some others) have proposed methods that prioritize “representative” data points, often built on clustering methods such as k -means. These methods can work substantially better in low-budget regimes, but themselves often saturate performance and do worse than uncertainty-based selection once budgets are large enough.

In practice it is difficult to know whether a given budget is “high” or “low” for a particular problem; it greatly depends on the particular dataset and model architecture. Hachohen & Weinshall (2024)

*These authors contributed equally.

proposed an algorithm, SelectAL, to select whether to use a high- or low-budget method. This approach, however, assumes discrete budget regimes when there is often not a clear boundary, and because of the form of the algorithm is also unable to consider uncertainty-based active learning measures directly. SelectAL also requires re-training models many times, which may be computationally infeasible, and requires a nontrivial amount of data holdout for validation, an issue when budgets are low. Perhaps most importantly, the algorithm appears quite sensitive to small, subtle decisions; our attempts at replication¹ gave extremely inconsistent and unreliable estimates of the regime, overall yielding much worse performance than reported in the paper.

This motivates the aim of finding a single active learning algorithm which can seamlessly adapt from low- to high-budget regimes. While there have been various hybrid methods combining representation and uncertainty, we find in practice that none of these methods work well in low-budget settings. We therefore propose an objective called *uncertainty coverage*, adding a notion of uncertainty to the “generalized coverage” of Bae et al. (2024) and its greedy optimizer MaxHerding. We call greedy optimization of the empirical estimate of the uncertainty coverage Uncertainty Herding (UHerding); we prove UHerding nearly maximizes the true uncertainty coverage.

The uncertainty coverage agrees with the generalized coverage in one extreme setting of parameters, while agreeing with uncertainty measures in another. To naturally interpolate between those settings, we propose a simple method to adaptively and automatically adjust these parameters such that the objective moves itself from mostly representation-based to mostly uncertainty-based behavior. With this parameter adaptation scheme, we demonstrate that UHerding outperforms MaxHerding (and all other methods) in low-budget regimes, while also outperforming uncertainty sampling (and all other methods) in high-budget regimes, across several benchmark datasets (CIFAR-10 and -100, Tiny-ImageNet, DomainNet, and ImageNet) in both standard supervised and transfer learning settings. Furthermore, we describe how several existing hybrid active learning methods are closely related to UHerding, and confirm that our parameter adaptation schemes also benefit existing hybrid methods.

2 RELATED WORK AND BACKGROUND

The most common framework in active learning is pool-based active learning. At each step $t \in \{1, 2, \dots, T\}$, a labeled set $\mathcal{L}_t \subseteq \mathcal{X}$ is iteratively expanded by querying a set of new data points $\mathcal{S}_t = \{\mathbf{x}_b\}_{b=1}^{B_t}$ from an unlabeled pool of data points $\mathcal{U}_t, \subseteq \mathcal{X}$ where \mathcal{X} denotes the support set of the data distribution of interest. A model is then trained on the new \mathcal{L}_{t+1} . Usually, the most important component is determining which points to annotate.

Uncertainty-based Methods “Myopic” methods that rely only on a current model’s predictions include entropy (Wang & Shang, 2014), margin Scheffer et al. (2001), confidence, and posterior probability (Lewis & Catlett, 1994; Lewis & Gale, 1994). In the Bayesian setting, BALD (Gal et al., 2017; Kirsch et al., 2019) uses mutual information between labels and model parameters. BAIT (Ash et al., 2021) tries to select data points that minimize Bayes risk. Instead of using a snapshot of a trained model, Kye et al. (2023) exploit uncertainties computed in the process of model training.

Some models focus on “looking ahead” to predict how a data point will change the model. These include methods based on expected changes in model parameters (Settles, 2009; Settles et al., 2007; Ash et al., 2020), expected changes in model predictions (Freitag et al., 2014; Käding et al., 2016; 2018), and expected error reduction (Roy & McCallum, 2001; Zhu et al., 2003; Guo & Greiner, 2007). These approaches are primarily used with simple models like linear and Naïve Bayes models. For deep models, a neural tangent kernel-based linearization (Mohamadi et al., 2022) can be used, though it offers limited improvement over uncertainty sampling relative to its computational cost.

Representation-based Methods These methods select data points that represent (or cover) the data distribution. Traditional methods include k -means (Xu et al., 2003), medoids (Aghaee et al., 2016) and medians (Voevodski et al., 2012). Hacohen et al. (2022) show that selecting representative points is particularly helpful in low-budget regimes, and propose Typiclust, which selects the “most typical” points in each cluster. Bıyık et al. (2019) utilize determinantal point processes instead.

¹The authors have not publicly released code, though they indicated they plan to in private communication.

Another approach is to minimize distance between the labeled and unlabeled data distributions, whether kernel MMD (Chen et al., 2010), Wasserstein distance (Mahmood et al., 2022), or an estimate of the KL divergence tailored to transfer learning as in ActiveFT (Xie et al., 2023).

Sener & Savarese (2018) convert the objective of active learning into maximum coverage, proposing greedy k -center. Instead of finding the minimum radius to cover all data points, ProbCover (Yehuda et al., 2022) greedily select data points to cover the most data points with a fixed radius. While its performance is sensitive to the choice of radius (also difficult to set), MaxHerding (Bae et al., 2024) generalizes to a continuous notion of coverage, generalized coverage (or GCoverage), which is less sensitive to parameter choice. As we build directly on this method, we describe it in more detail.

GCoverage is defined in terms of a function $k : \mathcal{X} \times \mathcal{X} \times (\mathcal{X} \rightarrow \mathcal{V}) \rightarrow \mathbb{R}_{\geq 0}$, which computes a similarity between \mathbf{x} and \mathbf{x}' based on a feature mapping $g : \mathcal{X} \rightarrow \mathcal{V}$. Bae et al. (2024) mostly use the Gaussian kernel² $k_\sigma(\mathbf{x}, \mathbf{x}'; g) = \exp\left(-\|g(\mathbf{x}) - g(\mathbf{x}')\|^2 / \sigma^2\right)$ with g based on self-supervised feature extractors such as SimCLR (Chen et al., 2020). The GCoverage and its estimator are

$$C_{k_\sigma}(\mathcal{S}) := \mathbb{E}_{\mathbf{x}} \left[\max_{\mathbf{x}' \in \mathcal{S}} k_\sigma(\mathbf{x}, \mathbf{x}'; g) \right] \approx \frac{1}{N} \sum_{n=1}^N \left(\max_{\mathbf{x}' \in \mathcal{S}} k_\sigma(\mathbf{x}_n, \mathbf{x}'; g) \right) =: \widehat{C}_{k_\sigma}(\mathcal{S}) \text{ with } \mathbf{x}_n \in \mathcal{U}. \quad (1)$$

MaxHerding greedily maximizes the estimated GCoverage: $\mathbf{x}^* \in \arg \max_{\tilde{\mathbf{x}} \in \mathcal{U}} \widehat{C}_{k_\sigma}(\mathcal{L} \cup \{\tilde{\mathbf{x}}\})$. This is a $(1 - \frac{1}{e})$ approximation algorithm for optimizing the monotone submodular function \widehat{C}_{k_σ} .

Hybrid Methods These methods aim to select informative yet representative data points. Nguyen & Smeulders (2004); Donmez et al. (2007) use margin-based selection weighted by clustering scores. Settles & Craven (2008) weight uncertainty measures like entropy by cosine similarity. For neural networks, BADGE (Ash et al., 2020) uses k -means++ on loss gradient space, while ALFA-Mix (Parvaneh et al., 2022) applies k -means to uncertain points based on feature interpolation.

Since uncertainty and representation-based active learning approaches behave differently in different budget regimes, SelectAL (Hacohen & Weinshall, 2024) and TCM (Doucet et al., 2024) provide methods to decide when to switch from low-budget to high-budget methods. TCM provides some insights for a transition point, but their insights are based on extensive experimentation, and hard to generalize to different settings. SelectAL was discussed in the previous section. In this work, we propose a more robust approach with minimal re-training, covering continuous budget regimes.

Clustering in active learning k -means is widely used in active learning to promote diversity in selection. BADGE, ALFA-Mix, and Typiclust, for example, use k -means or variants.

k -means centroids, however, do not in general correspond to any available point, and thus other methods (such as Typiclust’s density criterion) must be used to choose a point from a cluster. It would be natural to instead enforce centroids to be data points, yielding k -medoids. The common alternating update scheme similar to k -means often leads to poor local optima (Schubert & Rousseeuw, 2021). The Partitioning Around Medoids (PAM) algorithm (Kaufman & Rousseeuw, 2009; Schubert & Rousseeuw, 2019; Schubert & Lenssen, 2022) gives better clusters, but is much slower. MaxHerding selects points with essentially equivalent downstream performance as using the far more expensive Faster PAM algorithm (Schubert & Rousseeuw, 2021) for GCoverage.

As we demonstrate empirically in Figure 8b, MaxHerding achieves significantly better performance than both k -means and k -means++ for active learning. Thus, in Section 3.4, we replace k -means with MaxHerding for the theoretical analysis of some clustering-based active learning methods.

3 METHOD

We introduce a novel approach called Uncertainty Herding (UHerding), designed to “interpolate” between the state-of-the-art representation-based method MaxHerding and any choice of uncertainty-based method (*e.g.*, Margin), providing effectiveness across different budget regimes.

²Although we call the function k_σ and use the term “kernel,” it is not generally necessary that the function be positive semi-definite as in kernel methods, nor that it integrate to 1 as in kernel density estimation.

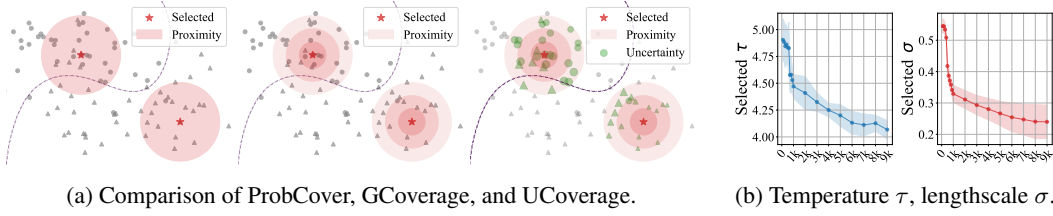


Figure 1: Left: illustration of coverages (Section 3.1). Right: parameter adaptation (Section 3.2).

3.1 UNCERTAINTY COVERAGE

We first define a measure of how much uncertainty a set of data points covers.

Definition 1. For any subset $\mathcal{S} \subset \mathcal{X}$, a nonnegative-valued function k_σ ,³ and nonnegative-valued uncertainty function U , *uncertainty coverage* (UCoverage) is defined and empirically estimated as

$$\text{UC}_{k_\sigma}(\mathcal{S}) = \mathbb{E}_{\mathbf{x}} \left[U(\mathbf{x}; f) \max_{\mathbf{x}' \in \mathcal{S}} k_\sigma(\mathbf{x}, \mathbf{x}'; g) \right] \approx \frac{1}{N} \sum_{n=1}^N U(\mathbf{x}_n; f) \max_{\mathbf{x}' \in \mathcal{S}} k_\sigma(\mathbf{x}_n, \mathbf{x}'; g) = \widehat{\text{UC}}_{k_\sigma}(\mathcal{S}).$$

Here, the uncertainty function U is based on a model f which is updated as the model trains, while k_σ uses a fixed feature extractor g . UCoverage weights the GCoverage of (1) with a choice of uncertainty measure $U(\mathbf{x}; f)$; choosing $U(\mathbf{x}; f) = 1$ immediately recovers GCoverage.

In Figure 1a, we visualize differences in assessing coverage. ProbCover (left) treats all data points within a σ -radius ball around selected points equally, assigning uniform weight to each. GCover (middle) introduces a smooth proximity measure by applying a kernel function, such as the RBF kernel, to weigh nearby points more effectively. UCover (right) additionally incorporates uncertainty. The green circles represent uncertainty, with their size proportional to each point’s uncertainty. Ultimately, UCover evaluates how well the selected data points account for uncertainty across the space.

We now show $\widehat{\text{UC}}_{k_\sigma}$ is a good estimator of UC_{k_σ} . All proofs are in Appendix A.

Theorem 2. Let $U(\mathbf{x}; f) \in [0, U_{\max}]$, $k_\sigma(\mathbf{x}, \mathbf{x}'; g) = \tilde{k}_\sigma(g(\mathbf{x}), g(\mathbf{x}')) \in [0, 1]$, $\{g(\mathbf{x}) : \mathbf{x} \in \mathcal{U}\} \subseteq \{\mathbf{t} \in \mathbb{R}^d : \|\mathbf{t}\| \leq R\}$, and $|\tilde{k}_\sigma(\mathbf{t}, \mathbf{t}') - \tilde{k}_\sigma(\mathbf{t}, \mathbf{t}'')| \leq L_\sigma \|\mathbf{t}' - \mathbf{t}''\|$. Let $\mathcal{L} \subseteq \mathcal{X}$ be arbitrary and fixed. Assume $B/N < 16R^2$. Then, with probability at least $1 - \delta$ over the choice of the N iid data points in $\mathcal{U} \subseteq \mathcal{X}$ used to estimate $\widehat{\text{UC}}_{k_\sigma}$, all size- B sets \mathcal{S} (not only subsets of \mathcal{U}) have low error:

$$\sup_{\substack{\mathcal{S} \subseteq \mathcal{X} \\ |\mathcal{S}|=B}} \left| \text{UC}_{k_\sigma}(\mathcal{L} \cup \mathcal{S}) - \widehat{\text{UC}}_{k_\sigma}(\mathcal{L} \cup \mathcal{S}) \right| \leq U_{\max} \sqrt{\frac{B}{N}} \left[8L_\sigma + \frac{1}{2} \sqrt{d \log \left(R^2 \frac{N}{B} \right) + \frac{2}{B} \log \frac{2}{\delta}} \right].$$

Since typically $B \ll N$ – we query up to perhaps a few hundred points at a time, out of a dataset of at least tens of thousands but perhaps millions – even optimizing our noisy estimate of the uncertainty coverage does not introduce substantial error.⁴ If U is given by the margin between probabilistic predictions, then $U_{\max} \leq 1$; other notions can also be easily bounded. Assuming $k_\sigma \leq 1$ is for convenience, but a different upper bound can simply be absorbed into U_{\max} . The bound is indeed 1 for the Gaussian kernel on g used by Bae et al. (2024) (as well as by us); this kernel also has $L_\sigma = \sqrt{\frac{2}{e}} \cdot \frac{1}{\sigma}$. The kernel which corresponds to the probability coverage of Yehuda et al. (2022), however, is not Lipschitz, suggesting why it is so sensitive to σ . Self-supervised representations in g are often normalized to $R = 1$, and usually have d at most a few hundred.

³We typically use $k_\sigma(\mathbf{x}, \mathbf{x}'; g) = \psi((g(\mathbf{x}) - g(\mathbf{x}'))/\sigma) \in [0, 1]$ for some function ψ and a feature map g .

⁴It is worth emphasizing that, although Bae et al. (2024) mentioned a simple Hoeffding bound for $\widehat{\text{C}}_{k_\sigma}$, this bound only applies to fixed \mathcal{S} independent of \mathcal{U} – while in reality $\mathcal{S} \subseteq \mathcal{U}$. Ignoring this problem and taking a union bound over all $\binom{N}{B}$ subsets of \mathcal{U} would yield a uniform convergence bound of $U_{\max} \sqrt{\frac{1}{2N} \log \left(\binom{N}{B} \frac{2}{\delta} \right)} \leq U_{\max} \sqrt{\frac{B}{2N}} \left[\log \left(e \frac{N}{B} \right) + \frac{1}{B} \log \frac{2}{\delta} \right]$. The rate of Theorem 2 is very similar, with the advantage of being correct.

Algorithm 1: Uncertainty herding with parameter adaptation

Input: Initial labeled set \mathcal{L}_0 , Initial unlabeled set \mathcal{U}_0 , a set of temperatures \mathcal{T} , the number of iterations T , a set of query budgets $\{B_t\}_{t=0}^{T-1}$, a classifier f , and a feature extractor g

```
1 for  $t \in [0, 1, \dots, T-1]$  do
  // Parameter adaptation
2   Compute  $\tau^* = \arg \min_{\tau \in \mathcal{T}} \text{ECE}(f^{\mathcal{L}_t^{\text{train}}}, \mathcal{L}_t^{\text{val}})$  where  $\mathcal{L}_t^{\text{train}}$  and  $\mathcal{L}_t^{\text{val}}$  are random split from
    $\mathcal{L}_t$ , and  $f^{\mathcal{L}_t^{\text{train}}}$  refers to a classifier  $f$  trained on  $\mathcal{L}_t^{\text{train}}$ 
3   Compute  $\mathbf{k} \in \mathbb{R}^{|\mathcal{U}_t|}$  with  $\mathbf{k}_n = \max_{\mathbf{x}' \in \mathcal{L}_t} k_{\sigma^*}(\mathbf{x}_n, \mathbf{x}')$  for  $\sigma^* = \min_{\mathbf{u}, \mathbf{v} \in \mathcal{L}_t, \mathbf{u} \neq \mathbf{v}} D(\mathbf{u}, \mathbf{v}; g)$ 
  // Greedy selection based on the uncertainty coverage
4   for  $b \in [1, 2, \dots, B_t]$  do
5     Select  $\mathbf{x}_b^* = \arg \max_{\tilde{\mathbf{x}} \in \mathcal{U}} \frac{1}{N} \sum_{n=1}^N U(x_n; f_{\tau^*}) \cdot \max(k_{\sigma^*}(\mathbf{x}_n, \tilde{\mathbf{x}}) - \mathbf{k}_n, 0)$ 
6     Update  $\mathbf{k}_n \leftarrow \max(k_{\sigma^*}(\mathbf{x}_n, \mathbf{x}_b^*), \mathbf{k}_n), \forall n \in |\mathcal{U}_t|$ 
7   Update  $\mathcal{L}_{t+1} \leftarrow \mathcal{L}_t \cup \{\mathbf{x}_b^*\}_{b=1}^{B_t}$  and  $\mathcal{U}_{t+1} \leftarrow \mathcal{U}_t \setminus \{\mathbf{x}_b^*\}_{b=1}^{B_t}$ 
```

3.2 PARAMETER ADAPTATION

We wish to choose parameters of UCoverage such that it smoothly changes from behaving like generalized coverage in low-budget regimes to behaving like uncertainty in high-budget regimes.

Handling the low-budget case: calibration When $|\mathcal{S}|$ is small, we would like to roughly replicate GCoverage. We can do this by making our uncertainty function constant:

Proposition 3. *If $\forall \mathbf{x} \in \mathcal{U}, U(\mathbf{x}; f) \rightarrow c$ where $c \geq 0$, the estimated UCoverage $\widehat{\text{UC}}_{k_\sigma}(\mathcal{S})$ approaches the estimated GCoverage $\widehat{\text{C}}_{k_\sigma}(\mathcal{S})$, up to a constant.*

When $|\mathcal{L}|$ is very small, our model f is bad. Models with poor predictive power will generally have near-constant uncertainty if they are well-calibrated. We thus encourage calibration primarily through temperature scaling, a simple but effective post-hoc calibration method (Guo et al., 2017):

1. Split \mathcal{L}_t into $\mathcal{L}_t^{\text{train}}$ and $\mathcal{L}_t^{\text{val}}$, and train a model f on $\mathcal{L}_t^{\text{train}}$, obtaining $f^{\mathcal{L}_t^{\text{train}}}$.
2. Choose τ^* among some candidate set \mathcal{T} to minimize the expected calibration error (ECE) (Naeni et al., 2015) of the temperature-scaled predictions $f(\mathbf{x})/\tau$ on $\mathcal{L}_t^{\text{val}}$. Here $f(\mathbf{x}) \in \mathbb{R}^K$ denotes a logit vector, with K the number of classes.
3. Compute uncertainties with τ^* -scaled softmax: $\log \hat{p}_{\tau^*}(\mathbf{x}) \propto f_{\tau^*}(\mathbf{x}) := f(\mathbf{x})/\tau^*$.

The selected temperatures τ^* are generally large when $|\mathcal{L}|$ is small and so f has poor predictions, which makes $U(\mathbf{x}; f)$ close to constant. As $|\mathcal{L}|$ increases and f 's predictions improve, τ^* decreases (see Figure 1b, left panel), making uncertainty values more distinct.

Handling the high-budget case: decreasing σ As $|\mathcal{L}|$ increases, the effect of a single new data point on the trained model tends to become more “semantically local,” implying it is reasonable to treat points as “covering” only closer and closer points in g space by decreasing the radius σ . As a heuristic, we choose the radius to be the minimum distance between data points in the labeled set \mathcal{L} : $\sigma^* = \min_{\mathbf{u}, \mathbf{v} \in \mathcal{L}, \mathbf{u} \neq \mathbf{v}} \|g(\mathbf{u}) - g(\mathbf{v})\|$. Since \mathcal{U} is bounded, as $|\mathcal{L}|$ grows we have that $\sigma^* \rightarrow 0$ (see Figure 1b, right panel); thus Proposition 4 eventually applies, becoming uncertainty-based selection.

Proposition 4. *Suppose $k_\sigma(\mathbf{x}, \mathbf{x}'; g) = \psi((g(\mathbf{x}) - g(\mathbf{x}'))/\sigma)$ for a fixed $g : \mathcal{X} \rightarrow \mathbb{R}^d$ which is injective on \mathcal{U} , and a function $\psi : \mathbb{R}^d \rightarrow [0, 1]$ with $\psi(0) = 1$ and for all $t \in \mathbb{R}^d$ with $\|t\| = 1, \lim_{a \rightarrow \infty} \psi(at) = 0$. If $\sigma \rightarrow 0$, the estimated uncertainty coverage $\widehat{\text{UC}}_{k_\sigma}(\mathcal{S})$ approaches $\sum_{s=1}^{|\mathcal{S}|} U(\mathbf{x}_s; f)$, up to a constant.*

As we shall see in Section 4.4, UCoverage with fixed τ and σ is not robust across budget levels, performing worse than MaxHerding in low-budget and worse than Margin in high-budget regimes. With our adaption techniques, however, UCoverage outperforms competitors across label budgets.

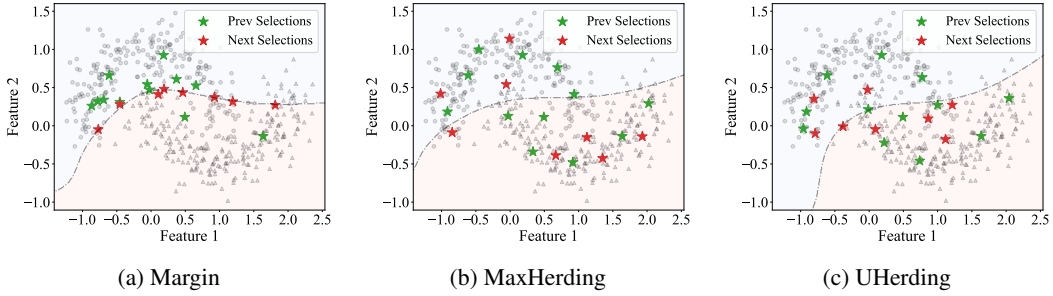


Figure 2: Comparison of Margin, MaxHerding and proposed UHerding on half-moon toy data.

3.3 UNCERTAINTY HERDING

To obtain an actual active learning method, we still need an algorithm to maximize \widehat{UC}_{k_σ} . We could select a batch by finding $\widehat{S} \in \arg \max_{S \subseteq \mathcal{U}, |S|=B} \widehat{UC}_{k_\sigma}(\mathcal{L} \cup S)$. This is equivalent to the weighted kernel k -medoids objective, with weights determined by uncertainty $U(\mathbf{x}; f)$; thus, we could use Partitioning Around Medoids (PAM) (Kaufman & Rousseeuw, 2009) to try to find \widehat{S} .

Bae et al. (2024), however, observed that even with a highly optimized implementation, this algorithm is much slower to optimize GCoverage than greedy methods, with little improvement in active learning performance. We thus focus on greedy selection, which we call Uncertainty Herding (UHerding) by analogy to MaxHerding (itself an analogy to kernel herding, Chen et al., 2010).

Definition 5 (Uncertainty Herding). To greedily add a single data point to a set $\mathcal{L}' = \mathcal{L} \cup S$, select

$$\mathbf{x}^* \in \arg \max_{\tilde{\mathbf{x}} \in \mathcal{U}} \widehat{UC}_{k_\sigma}(\mathcal{L}' \cup \{\tilde{\mathbf{x}}\}) = \arg \max_{\tilde{\mathbf{x}} \in \mathcal{U}} \left(\frac{1}{N} \sum_{n=1}^N U(\mathbf{x}_n; f_\tau) \cdot \max_{\mathbf{x}' \in \mathcal{L}' \cup \{\tilde{\mathbf{x}}\}} k_\sigma(\mathbf{x}_n, \mathbf{x}'; g) \right). \quad (2)$$

UHerding selects a new batch S of size $|S|$ by picking one point at a time to add to \mathcal{L}' .

UHerding improves uncertainty measures by accounting for both the uncertainty of a selected point and its influence on reducing nearby uncertainty. It improves on MaxHerding by incorporating uncertainty, putting less weight on covering already-certain points.

Corollary 6. In the setting of Theorem 2, let $\widehat{S} \subseteq \mathcal{U}$ be the result of UHerding for B steps to add to \mathcal{L} , and $UC^* = \max_{S \subseteq \mathcal{U}, |S|=B} UC_{k_\sigma}(\mathcal{L} \cup S)$ the optimal coverage obtainable among \mathcal{U} . Then

$$UC_{k_\sigma}(\mathcal{L} \cup \widehat{S}) \geq \left(1 - \frac{1}{e}\right) UC^* - \left(2 - \frac{1}{e}\right) U_{\max} \sqrt{\frac{B}{N}} \left[8L_\sigma + \frac{1}{2} \sqrt{d \log \left(R^2 \frac{N}{B} \right) + \frac{2}{B} \log \frac{2}{\delta}} \right].$$

Figure 2 visually compares the next selected data points (in red) by Margin, MaxHerding, and UHerding (using Margin uncertainty) on a two-class half-moon dataset represented by \circ and \triangle . A logistic regression model with fifth-order polynomial features is trained at each iteration, with the decision boundary after training on 12 previously selected points (in green) shown as dashed lines. As expected, Margin selects points near the decision boundary, which can lead to suboptimal models if the predicted boundary deviates from the true one. MaxHerding selects the most representative points based on prior selections but ignores model predictions; this gives quick generalization with few labeled points, but performance saturates over time as it neglects points near the boundary. UHerding balances these approaches by initially selecting representative points and gradually focusing on uncertain points near the boundary, improving performance over time.

3.4 CONNECTION TO HYBRID METHODS

UHerding is closely connected to existing hybrid active learning methods. As mentioned in Section 2, we replace k -means and k -means++ in various algorithms with greedy kernel k -medoids (MaxHerding) to simplify our arguments; this does not harm their effectiveness. We also apply a self-supervised feature extractor g instead of a feature extractor from a classifier f , since feature

embeddings from g are more informative when f is trained on a small labeled set. Finally, we often assume that k_σ is in fact a positive-definite (RKHS) kernel; this is true for the kernels we use.

Proposition 7 (Weighted k -means of Zhdanov 2019). *Define an uncertainty measure $U(\mathbf{x}; f)$ from another uncertainty measure $U'(\mathbf{x}; f)$ as $U(\mathbf{x}; f) := U'(\mathbf{x}; f) \cdot \mathbb{1}[U'(\tilde{\mathbf{x}}; f) \geq \nu]$, where $\nu \geq 0$ satisfies $\sum_{n=1}^N \mathbb{1}[U'(\mathbf{x}_n; f) \geq \nu] = M$, a pre-defined number. Then weighted k -means with uncertainty U' , changed to use greedy kernel k -medoids, is UHerding with uncertainty U and the same kernel.*

As we shall see in Section 4, UHerding significantly outperforms weighted k -means, indicating that it is crucial to (a) convert k -means into MaxHerding and (b) apply parameter adaptation.

Proposition 8 (ALFA-Mix of Parvaneh et al. 2022). *Let $\hat{y}(\cdot; f)$ be the predicted label of an input under f . Define an uncertainty measure*

$$U(\mathbf{x}; f) := \mathbb{1}[\exists \text{ class } j \text{ s.t. } \hat{y}(\alpha_j(\mathbf{x})g(\mathbf{x}) + (1 - \alpha_j(\mathbf{x}))\bar{g}_j; f) \neq \hat{y}(g(\mathbf{x}); f)] \quad (3)$$

where \bar{g}^j is the mean of feature representations belonging to class j and $\alpha_j(\mathbf{x}) \in [0, 1]$ is the same parameter as determined by ALFA-Mix. Then ALFA-Mix, with clustering replaced by greedy kernel k -medoids, is UHerding with uncertainty U and the same kernel.

The equivalence of weighted k -means and ALFA-Mix to UHerding with the right choice of uncertainty measure implies that Propositions 3 and 4 also apply to them. There is a weaker connection to BADGE; UHerding and BADGE are not equivalent with any choice of uncertainty measure. However, a variant of BADGE with greedy kernel k -medoids uses the kernel,

$$h(\mathbf{x}_n, \mathbf{x}') = 2\langle q(\mathbf{x}_n), q(\mathbf{x}') \rangle k_\sigma(\mathbf{x}_n, \mathbf{x}'; g) - \|q(\mathbf{x}_n)\|_2^2 k_\sigma(\mathbf{x}_n, \mathbf{x}_n; g) - \|q(\mathbf{x}')\|_2^2 k_\sigma(\mathbf{x}', \mathbf{x}'; g) \quad (4)$$

where $q(\mathbf{x}) = \hat{y}(\mathbf{x}; f) - \hat{p}(\mathbf{x}; f)$ with f being a classifier. This does satisfy the following statement, showing properties similar to Propositions 3 and 4 hold.

Proposition 9 (BADGE, Ash et al., 2020). *If $\forall \mathbf{x} \in \mathcal{U}, \hat{p}(\mathbf{x}; f) \rightarrow \frac{1}{K} \vec{1}$, then this BADGE approaches a slightly modified MaxHerding: $(\mathbb{1}[\hat{y}(\mathbf{x}_n; f) = \hat{y}(\mathbf{x}'; f)] - \frac{1}{K}) k_\sigma(\mathbf{x}_n, \mathbf{x}'; g)$ instead of $k_\sigma(\mathbf{x}_n, \mathbf{x}'; g)$. If $\sigma \rightarrow 0$, it approaches to the uncertainty-based method where uncertainty is defined as $U''(\tilde{\mathbf{x}}) := \min_{\mathbf{x}' \in \mathcal{L} \cup \{\tilde{\mathbf{x}}\}} \|\hat{y}(\mathbf{x}'; f) - \hat{p}(\mathbf{x}'; f)\|_2^2$.*

With our parameter adaptation heuristics, hybrid methods can also smoothly interpolate between MaxHerding and uncertainty; Figure 6b shows this improves BADGE. Although selecting data points maximizing $U''(\tilde{\mathbf{x}})$ is counter-intuitive, lowering σ still helps, as it stays away from zero.

4 EXPERIMENTS

In this section, we assess the robustness of the proposed UHerding against existing active learning methods for standard supervised learning (Sections 4.1 and 4.2) and transfer learning (Section 4.3) across several benchmark datasets: CIFAR10 (Krizhevsky, 2009), CIFAR100 (Krizhevsky et al.), TinyImageNet (mnmostafa, 2017), ImageNet (Deng et al., 2009), and DomainNet (Peng et al., 2019). Section 4.4 gives ablation studies to see how each component of UHerding contributes.

Active learning methods We compare with several active learning methods listed below. We exclude ProbCover; its generalization MaxHerding reliably outperforms it (Bae et al., 2024).

Random Uniformly select random B data points from \mathcal{U} .

Confidence Iteratively select $\mathbf{x}^* \in \arg \min_{\tilde{\mathbf{x}} \in \mathcal{U}} p_1(y|\tilde{\mathbf{x}})$, with p_1 the highest predicted probability.

Margin Iteratively select $\mathbf{x}^* = \arg \min_{\tilde{\mathbf{x}} \in \mathcal{U}} p_1(y|\tilde{\mathbf{x}}) - p_2(y|\tilde{\mathbf{x}})$, where p_2 is the second-highest predicted probability (Scheffer et al., 2001).

Entropy Iteratively select $\mathbf{x}^* = \arg \max_{\tilde{\mathbf{x}} \in \mathcal{U}} H(\hat{y}(\tilde{\mathbf{x}}) | \tilde{\mathbf{x}})$, where $H(\cdot)$ is the Shannon entropy (Wang & Shang, 2014).

Weighted Entropy Select points closest to the centroids of weighted k -means using unlabeled data points with high enough margins (as in Margin selection above) (Zhdanov, 2019).

BADGE Select points with the k -means++ initialization algorithm using gradient embeddings w.r.t. the weights of the last layer (Ash et al., 2020).

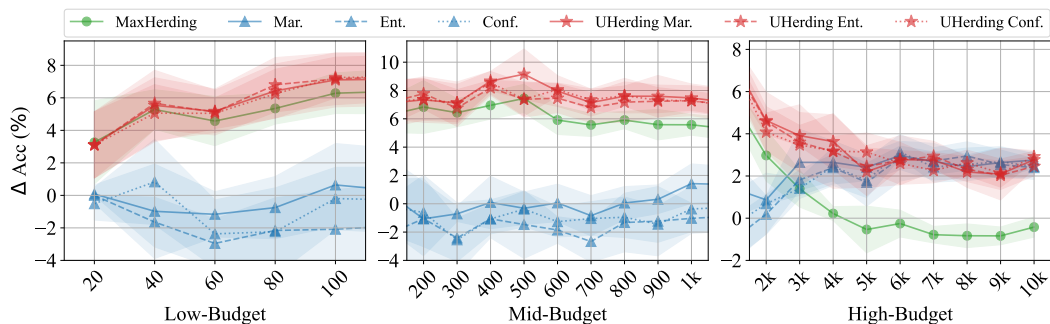


Figure 3: UHerding versus MaxHerding and uncertainty, with different uncertainty measures. Mean and standard deviation of 5 runs of the difference between a method and Random selection.

ALFA-Mix Select data points closest to the centroids of k -means only using uncertain unlabeled data points, based on feature interpolation (Parvaneh et al., 2022).

ActiveFT Select data points close to parameterized “centroids,” learned by minimizing KL between the unlabeled set and selected set, along with diversity regularization (Xie et al., 2023).

Typiclust Run a clustering algorithm, *e.g.*, k -means. For each cluster, select a point with the highest “typicality” using m -Nearest Neighbors (Hacohen et al., 2022).

Coreset Iteratively select points with k -Center-Greedy algorithm (Sener & Savarese, 2018):

$$\mathbf{x}^* = \arg \max_{\tilde{\mathbf{x}} \in \mathcal{U}} \min_{\mathbf{x}' \in \mathcal{L}} \|\tilde{\mathbf{x}} - \mathbf{x}'\|_2.$$

MaxHerding Iteratively select points to maximize the generalized coverage (1) (Bae et al., 2024).

Implementation We always re-initialize models (cold-start), randomly or from pre-trained parameters, after each round of acquisition, rather than warm-starting from the previous model (Ash & Adams, 2020). We manually categorize the budget regimes into low, mid, and high for supervised learning, and low and high for transfer learning tasks. Representation-based methods win in low-budget regimes, while uncertainty-based begin to catch up in mid-budget, and win in high-budget.

4.1 UHERDING INTERPOLATES, AND THE UNCERTAINTY MEASURE DOESN’T MATTER

We first aim to verify that UHerding effectively interpolates between MaxHerding and uncertainty measures across budget regimes. We train a randomly-initialized ResNet18 (He et al., 2016) on CIFAR10 using 5 random seeds, gradually increasing the size of the labeled set, as shown in Figure 3. We consider UHerding based on Margin (Mar.), Entropy (Ent.), and Confidence (Conf.). The y-axis of Figure 3 represents ΔAcc , indicating the performance difference from Random selection.

UHerding performs slightly better or comparably to MaxHerding in the low-budget regime, with a growing performance gap in the mid-budget regime, and substantial improvements in the high-budget regime. The opposite is true with uncertainty measures: UHerding is substantially better with low budgets, while they eventually catch up and tie UHerding with high budgets.

The choice of uncertainty measure has little impact on performance. We thus only use Margin as the UHerding uncertainty measure in the future unless otherwise specified.

4.2 COMPARISON WITH STATE OF THE ART

We now compare UHerding with state-of-the-art active learning methods, particularly hybrids, to assess their robustness across different budget regimes. Figure 4 compares CIFAR100 and TinyImagenet, using 3 runs of a randomly initialized ResNet18; CIFAR10 results are in Appendix B.

Overall trends are similar to before: representation-based methods are good with low budgets but lose as the budget increases; uncertainty-based and hybrid methods are largely the opposite. UHerding with Margin uncertainty (UHerding Mar.) wins convincingly: no competitor ever outperforms UHerding, and for each competitor there is some budget where UHerding wins substantially.

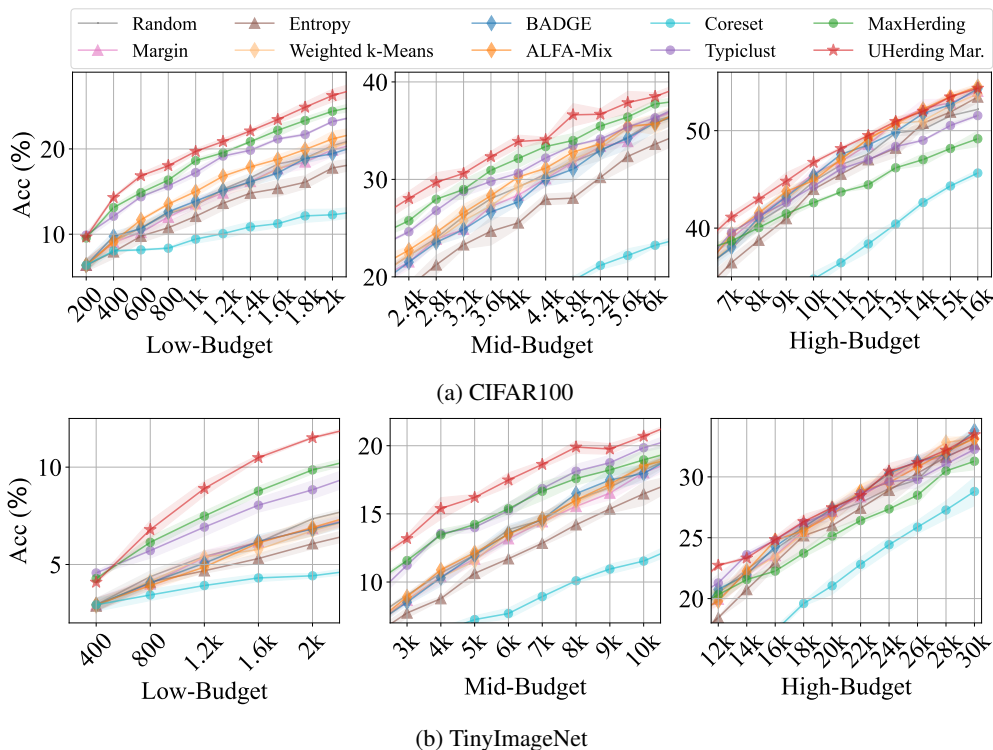


Figure 4: Comparison on CIFAR100 and TinyImageNet for supervised-learning tasks.

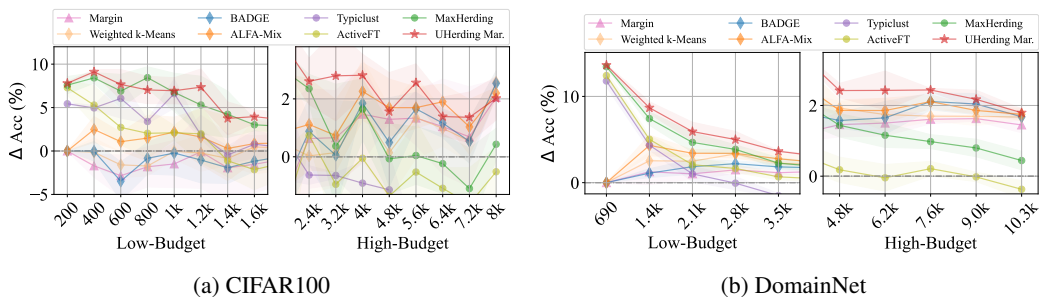


Figure 5: Comparison on CIFAR100 and DomainNet for transfer learning tasks.

4.3 COMPARISON FOR TRANSFER LEARNING TASKS

Fine-tuning foundation models to new tasks or datasets is of increasing importance. Inspired by ActiveFT (Xie et al., 2023), we compare UHerding to leading approaches for active transfer learning.

We use DeiT (Touvron et al., 2021) pre-trained on ImageNet (Deng et al., 2009), following Parvaneh et al. (2022); Xie et al. (2023). We fine-tune the entire model, using DeiT Small for CIFAR-100 and DeiT Base for DomainNet. Figure 5 compares UHerding with various active learning methods, including ActiveFT, which consistently underperforms the other methods likely due to its design being optimized for single-iteration data selection. On CIFAR100, UHerding is comparable to representation-based methods in the low-budget regime but surpasses them by about 2% in the high-budget; it substantially outperforms uncertainty and hybrid methods in the low-budget regime and ties or wins with high-budgets. On DomainNet, UHerding outperforms MaxHerding by 1.5–2% even in the low-budget. Compared to the best-performing hybrid method ALFA-Mix, UHerding wins by up to 13% with low budgets and performs similarly with high budgets.

It is also common to fine-tune only the last few layers, especially in meta-learning (Wang et al., 2019; Chen et al., 2019; Goldblum et al., 2020) and self-supervised learning (Chen et al., 2020; Caron et al., 2021). Similarly to Bae et al. (2024), we use DINO (Caron et al., 2021) features fixed through fine-

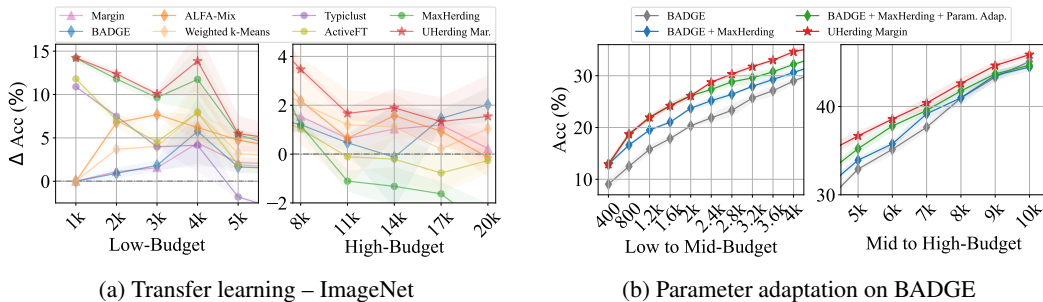


Figure 6: (Left) results on ImageNet for fine-tuning, (Right) application of parameter adaptation.

Method	Low					Middle			High				
	C10	C100	Tiny.	Dom.	ImN.	C10	C100	Tiny.	C10	C100	Tiny.	Dom.	ImN.
Entropy	-1.8	-1.7	-0.6	-0.2	1.7	-1.6	-2.9	-1.7	2.2	-0.6	-0.7	0.7	1.2
Margin	-0.4	-0.3	-0.2	1.0	1.8	-0.1	-0.4	-0.3	2.5	1.1	0.0	1.5	0.9
BADGE	-0.5	-0.1	-0.2	1.4	2.0	0.6	-0.7	0.0	2.2	0.9	0.4	1.8	1.0
ALFA-M	0.1	0.9	-0.3	2.8	5.1	1.1	0.6	0.1	2.3	1.3	0.2	1.9	1.0
Weight. k	-0.5	-0.1	-0.3	2.1	3.8	0.9	0.0	-0.2	1.8	0.8	0.3	1.7	0.8
Coreset	-2.7	-4.5	-1.4	-3.5	-6.6	-13	-11	-5.4	-10	-9.6	-5.5	-2.7	-12
ActiveFT	–	–	–	4.4	6.6	–	–	–	–	–	–	0.0	-0.1
Typiclust	3.7	3.3	1.6	3.1	4.9	4.9	1.8	2.1	-0.8	-0.1	0.3	-3.2	-9.9
MaxHerd.	5.0	4.1	2.1	6.2	10.6	6.2	2.8	1.9	0.1	-2.2	-1.5	1.0	-1.2
UHerding	5.5	5.5	3.1	7.4	11.2	7.8	4.3	3.7	3.0	2.1	0.8	2.3	2.0

Table 1: Comparison of the mean improvement/degradation over Random selection on each budget regime and dataset. The **first**, **second**, **third** best results for each setting are marked.

tuning; we train a head of three fully connected ReLU layers on ImageNet. Figure 6a shows similar results, with UHerding consistently outperforming other methods across various budget regimes.

Table 1 summarizes the results of Sections 4.2 and 4.3 and Appendix B, reporting the mean improvement/degradation over Random for each budget regime.⁵ UHerding wins across all budget regimes, while other methods have a significant range of budgets where they are worse than Random.

4.4 ABLATION STUDY

Figure 6b gradually modifies BADGE to be similar to UHerding with Margin uncertainty on CIFAR-100, replacing k -means++ with MaxHerding, then adding parameter adaptation. Each step improves; so does the final step to UHerding, which changes the choice of uncertainty.

In Appendix C, we analyze the contributions of each parameter adaptation component in UHerding. The baseline with fixed parameters performs slightly worse than MaxHerding at low- and mid-budgets, and worse than Margin at high-budgets. Adding temperature scaling results in notable improvements across all budget regimes, with further gains from incorporating radius adaptation.

5 CONCLUSION

In this work, we introduced uncertainty coverage, an objective that unifies low- and high-budget active learning objectives through a smooth interpolation with adaptive parameter adjustments. We showed generalization guarantees for the optimization of this coverage. By identifying conditions under which uncertainty coverage approaches generalized coverage and uncertainty measures, we made UHerding robust across various budget regimes. This adaptation also enhances an existing hybrid active learning method when similar parameter adjustments are applied. UHerding achieves state-of-the-art performance across various active learning and transfer learning tasks and, to our knowledge, is the only method that consistently performs well in both low- and high-budget settings.

⁵ ActiveFT is reported only for DomainNet (Dom.) and ImageNet (ImN.), as it is designed for fine-tuning.

ACKNOWLEDGMENTS

This work was supported in part by Mitacs through the Mitacs Accelerate program, the Natural Sciences and Engineering Research Council of Canada, the Canada CIFAR AI chairs program, and Advanced Research Computing at the University of British Columbia.

REFERENCES

- Amin Aghaee, Mehrdad Ghadiri, and Mahdiah Soleymani Baghshah. Active distance-based clustering using k-medoids. In *PAKDD*, 2016.
- Jordan Ash and Ryan P Adams. On warm-starting neural network training. In *NeurIPS*, 2020.
- Jordan Ash, Surbhi Goel, Akshay Krishnamurthy, and Sham Kakade. Gone fishing: Neural active learning with fisher embeddings. 2021.
- Jordan T Ash, Chicheng Zhang, Akshay Krishnamurthy, John Langford, and Alekh Agarwal. Deep batch active learning by diverse, uncertain gradient lower bounds. In *ICLR*, 2020.
- Wonho Bae, Junhyug Noh, and Danica J Sutherland. Generalized coverage for more robust low-budget active learning. In *ECCV*, 2024.
- Erdem Bıyık, Kenneth Wang, Nima Anari, and Dorsa Sadigh. Batch active learning using determinantal point processes. In *NeurIPS*, 2019.
- Mathilde Caron, Hugo Touvron, Ishan Misra, Hervé Jégou, Julien Mairal, Piotr Bojanowski, and Armand Joulin. Emerging properties in self-supervised vision transformers. In *ICCV*, 2021.
- Ting Chen, Simon Kornblith, Mohammad Norouzi, and Geoffrey Hinton. A simple framework for contrastive learning of visual representations. In *ICML*, 2020.
- Wei-Yu Chen, Yen-Cheng Liu, Zsolt Kira, Yu-Chiang Frank Wang, and Jia-Bin Huang. A closer look at few-shot classification. In *ICLR*, 2019.
- Yutian Chen, Max Welling, and Alex Smola. Super-samples from kernel herding. In *UAI*, 2010.
- Felipe Cucker and Steve Smale. On the mathematical foundations of learning. *Bulletin of the American Mathematical Society*, 2001.
- Jia Deng, Wei Dong, Richard Socher, Li-Jia Li, Kai Li, and Li Fei-Fei. ImageNet: A large-scale hierarchical image database. In *CVPR*, 2009.
- Pinar Donmez, Jaime G Carbonell, and Paul N Bennett. Dual strategy active learning. In *ECML*, 2007.
- Paul Doucet, Benjamin Estermann, Till Aczel, and Roger Wattenhofer. Bridging diversity and uncertainty in active learning with self-supervised pre-training. In *ICLR Workshop*, 2024.
- Alexander Freytag, Erik Rodner, and Joachim Denzler. Selecting influential examples: Active learning with expected model output changes. In *ECCV*, 2014.
- Yarin Gal, Riashat Islam, and Zoubin Ghahramani. Deep bayesian active learning with image data. In *ICML*, 2017.
- Micah Goldblum, Steven Reich, Liam Fowl, Renkun Ni, Valeriia Cherepanova, and Tom Goldstein. Unraveling meta-learning: Understanding feature representations for few-shot tasks. In *ICML*, 2020.
- Chuan Guo, Geoff Pleiss, Yu Sun, and Kilian Q Weinberger. On calibration of modern neural networks. In *ICML*, 2017.
- Yuhong Guo and Russell Greiner. Optimistic active-learning using mutual information. In *IJCAI*, 2007.

-
- Guy Hacohen and Daphna Weinshall. How to select which active learning strategy is best suited for your specific problem and budget. In *NeurIPS*, 2024.
- Guy Hacohen, Avihu Dekel, and Daphna Weinshall. Active learning on a budget: Opposite strategies suit high and low budgets. In *ICML*, 2022.
- Kaiming He, Xiangyu Zhang, Shaoqing Ren, and Jian Sun. Deep residual learning for image recognition. In *CVPR*, 2016.
- Christoph Käding, Erik Rodner, Alexander Freytag, and Joachim Denzler. Active and continuous exploration with deep neural networks and expected model output changes. In *NIPSW*, 2016.
- Christoph Käding, Erik Rodner, Alexander Freytag, Oliver Mothes, Björn Barz, Joachim Denzler, and Carl Zeiss AG. Active learning for regression tasks with expected model output changes. In *BMVC*, 2018.
- Leonard Kaufman and Peter J Rousseeuw. *Finding groups in data: an introduction to cluster analysis*. John Wiley & Sons, 2009.
- Andreas Kirsch, Joost Van Amersfoort, and Yarin Gal. Batchbald: Efficient and diverse batch acquisition for deep bayesian active learning. In *NeurIPS*, 2019.
- Alex Krizhevsky. Learning multiple layers of features from tiny images, 2009.
- Alex Krizhevsky, Vinod Nair, and Geoffrey Hinton. Cifar-100 (canadian institute for advanced research). URL <http://www.cs.toronto.edu/~kriz/cifar.html>.
- Seong Min Kye, Kwanghee Choi, Hyeongmin Byun, and Buru Chang. Tidal: Learning training dynamics for active learning. In *ICCV*, 2023.
- David D Lewis and Jason Catlett. Heterogeneous uncertainty sampling for supervised learning. In *Machine learning proceedings*, 1994.
- David D Lewis and William A Gale. A sequential algorithm for training text classifiers. In *SIGIR*, 1994.
- Rafid Mahmood, Sanja Fidler, and Marc T Law. Low budget active learning via wasserstein distance: An integer programming approach. In *ICLR*, 2022.
- Mohammed Ali mnmoustafa. Tiny imagenet, 2017. URL <https://kaggle.com/competitions/tiny-imagenet>.
- Mohamad Amin Mohamadi, Wonho Bae, and Danica J Sutherland. Making look-ahead active learning strategies feasible with neural tangent kernels. In *NeurIPS*, 2022.
- Mahdi Pakdaman Naeini, Gregory Cooper, and Milos Hauskrecht. Obtaining well calibrated probabilities using bayesian binning. In *AAAI*, 2015.
- G. L. Nemhauser, L. A. Wolsey, and M. L. Fisher. An analysis of approximations for maximizing submodular set functions—i. *Mathematical Programming*, 1978.
- Hieu T Nguyen and Arnold Smeulders. Active learning using pre-clustering. In *ICML*, 2004.
- Amin Parvaneh, Ehsan Abbasnejad, Damien Teney, Gholamreza Reza Haffari, Anton Van Den Hengel, and Javen Qinfeng Shi. Active learning by feature mixing. In *CVPR*, 2022.
- Xingchao Peng, Qinxun Bai, Xide Xia, Zijun Huang, Kate Saenko, and Bo Wang. Moment matching for multi-source domain adaptation. In *ICCV*, 2019.
- Nicholas Roy and Andrew McCallum. Toward optimal active learning through monte carlo estimation of error reduction. In *ICML*, 2001.
- Tobias Scheffer, Christian Decomain, and Stefan Wrobel. Active hidden Markov models for information extraction. In *ISIDA*, 2001.

-
- Erich Schubert and Lars Lenssen. Fast k-medoids clustering in Rust and Python. *Journal of Open Source Software*, 2022.
- Erich Schubert and Peter J Rousseeuw. Faster k-medoids clustering: improving the PAM, CLARA, and CLARANS algorithms. In *Similarity Search and Applications: 12th International Conference, SISAP 2019, Newark, NJ, USA, October 2–4, 2019, Proceedings 12*, 2019.
- Erich Schubert and Peter J Rousseeuw. Fast and eager k-medoids clustering: O(k) runtime improvement of the PAM, CLARA, and CLARANS algorithms. *Information Systems*, 2021.
- Ozan Sener and Silvio Savarese. Active learning for convolutional neural networks: A core-set approach. In *ICLR*, 2018.
- Burr Settles. Active learning literature survey. University of Wisconsin-Madison Department of Computer Sciences, 2009.
- Burr Settles and Mark Craven. An analysis of active learning strategies for sequence labeling tasks. In *EMNLP*, 2008.
- Burr Settles, Mark Craven, and Soumya Ray. Multiple-instance active learning. 2007.
- Hugo Touvron, Matthieu Cord, Matthijs Douze, Francisco Massa, Alexandre Sablayrolles, and Hervé Jégou. Training data-efficient image transformers & distillation through attention. In *ICML*, 2021.
- Konstantin Voevodski, Maria-Florina Balcan, Heiko Röglin, Shang-Hua Teng, and Yu Xia. Active clustering of biological sequences. In *JMLR*, 2012.
- Dan Wang and Yi Shang. A new active labeling method for deep learning. In *IJCNN*, 2014.
- Yan Wang, Wei-Lun Chao, Kilian Q. Weinberger, and Laurens van der Maaten. Simpleshot: Revisiting nearest-neighbor classification for few-shot learning. *arXiv:1911.04623*, 2019.
- Yichen Xie, Han Lu, Junchi Yan, Xiaokang Yang, Masayoshi Tomizuka, and Wei Zhan. Active finetuning: Exploiting annotation budget in the pretraining-finetuning paradigm. In *CVPR*, 2023.
- Zhao Xu, Kai Yu, Volker Tresp, Xiaowei Xu, and Jizhi Wang. Representative sampling for text classification using support vector machines. In *ECIR*, 2003.
- Ofer Yehuda, Avihu Dekel, Guy Hacohen, and Daphna Weinshall. Active learning through a covering lens. In *NeurIPS*, 2022.
- Fedor Zhdanov. Diverse mini-batch active learning. *arXiv preprint arXiv:1901.05954*, 2019.
- Xiaojin Zhu, John Lafferty, and Zoubin Ghahramani. Combining active learning and semi-supervised learning using gaussian fields and harmonic functions. In *ICML Workshop*, 2003.

A PROOFS

A.1 ESTIMATION QUALITY

Theorem 2. Let $U(\mathbf{x}; f) \in [0, U_{\max}]$, $k_\sigma(\mathbf{x}, \mathbf{x}'; g) = \tilde{k}_\sigma(g(\mathbf{x}), g(\mathbf{x}')) \in [0, 1]$, $\{g(\mathbf{x}) : \mathbf{x} \in \mathcal{U}\} \subseteq \{\mathbf{t} \in \mathbb{R}^d : \|\mathbf{t}\| \leq R\}$, and $|\tilde{k}_\sigma(\mathbf{t}, \mathbf{t}') - \tilde{k}_\sigma(\mathbf{t}, \mathbf{t}'')| \leq L_\sigma \|\mathbf{t}' - \mathbf{t}''\|$. Let $\mathcal{L} \subseteq \mathcal{X}$ be arbitrary and fixed. Assume $B/N < 16R^2$. Then, with probability at least $1 - \delta$ over the choice of the N iid data points in $\mathcal{U} \subseteq \mathcal{X}$ used to estimate $\widehat{\text{UC}}_{k_\sigma}$, all size- B sets \mathcal{S} (not only subsets of \mathcal{U}) have low error:

$$\sup_{\substack{\mathcal{S} \subseteq \mathcal{X} \\ |\mathcal{S}|=B}} \left| \text{UC}_{k_\sigma}(\mathcal{L} \cup \mathcal{S}) - \widehat{\text{UC}}_{k_\sigma}(\mathcal{L} \cup \mathcal{S}) \right| \leq U_{\max} \sqrt{\frac{B}{N}} \left[8L_\sigma + \frac{1}{2} \sqrt{d \log \left(R^2 \frac{N}{B} \right) + \frac{2}{B} \log \frac{2}{\delta}} \right].$$

Proof. Rather than operating directly on sets $\mathcal{S} \subseteq \mathcal{X}$, we will operate on B -tuples $\mathcal{T} \in (\mathbb{R}^d)^B$ corresponding to $(g(\mathbf{s}_1), \dots, g(\mathbf{s}_B))$. As these are ordered tuples, the mapping from \mathcal{T} to \mathcal{S} is many-to-one even if g is injective; if we prove convergence for all \mathcal{T} , it will necessarily prove convergence for all \mathcal{S} . Define $F(\mathcal{T}) = \text{UC}_{k_\sigma}(\mathcal{L} \cup \mathcal{S})$ and $\hat{F}(\mathcal{T}) = \widehat{\text{UC}}_{k_\sigma}(\mathcal{L} \cup \mathcal{S})$ for any \mathcal{S} corresponding to that \mathcal{T} ; this is well-defined, since UC_{k_σ} depends on \mathcal{S} only through $\{g(\mathbf{s}) : \mathbf{s} \in \mathcal{S}\}$.

Now, we will construct a vector space for elements $\mathcal{T} = (\mathbf{t}_1, \dots, \mathbf{t}_B)$. Vector addition and scalar multiplication are defined elementwise, and a norm is defined as $\|\mathcal{T}\| = \max(\|\mathbf{t}_1\|, \dots, \|\mathbf{t}_B\|)$, where $\|\mathbf{t}_i\|$ is the standard Euclidean norm. This space is complete, and hence a Banach space of dimension Bd .

The uncertainty coverage $F(\mathcal{T})$ is Lipschitz with respect to the Banach space norm:

$$\begin{aligned} |F(\mathcal{T}) - F(\mathcal{T}')| &\leq \mathbb{E}_{\mathbf{x}} U(\mathbf{x}; f) \left| \max_{\mathbf{t} \in \{g(\tilde{\mathbf{x}}) : \tilde{\mathbf{x}} \in \mathcal{L}\} \cup \mathcal{T}} \tilde{k}_\sigma(g(\tilde{\mathbf{x}}), \mathbf{t}) - \max_{\mathbf{t}' \in \{g(\tilde{\mathbf{x}}) : \tilde{\mathbf{x}} \in \mathcal{L}\} \cup \mathcal{T}'} \tilde{k}_\sigma(g(\tilde{\mathbf{x}}), \mathbf{t}') \right| \\ &\leq \mathbb{E}_{\mathbf{x}} U(\mathbf{x}; f) \max_{i \in [B]} |\tilde{k}_\sigma(g(\mathbf{x}), \mathbf{t}_i) - \tilde{k}_\sigma(g(\mathbf{x}), \mathbf{t}'_i)| \\ &\leq \mathbb{E}_{\mathbf{x}} U(\mathbf{x}; f) \max_{i \in [B]} L_\sigma \|\mathbf{t}_i - \mathbf{t}'_i\| \\ &= L_\sigma (\mathbb{E}_{\tilde{\mathbf{x}}} U(\tilde{\mathbf{x}}; f)) \|\mathcal{T} - \mathcal{T}'\|. \end{aligned}$$

The second inequality holds because the maximum function is Lipschitz on \mathbb{R}^N . Specifically, let $a_1, \dots, a_N, a'_1, \dots, a'_N \in \mathbb{R}$, and let $\hat{n} \in \arg \max_{n \in [N]} a_n$. Then

$$\max_{n \in [N]} a_n - \max_{n \in [N]} a'_n = a_{\hat{n}} - \max_{n \in [N]} a'_n \leq a_{\hat{n}} - a'_{\hat{n}} \leq \max_{n \in [N]} a_n - a'_n \leq \max_{n \in [N]} |a_n - a'_n|,$$

and, symmetrically, it is at least $-\max |a_n - a'_n|$, so $|\max_n a_n - \max_n a'_n| \leq \max_n |a_n - a'_n|$.

As \hat{F} is exactly F with an empirical distribution for \mathbf{x} , it is $L_\sigma \left(\frac{1}{N} \sum_{n=1}^N U(\mathbf{x}_n) \right)$ -Lipschitz. We thus have

$$\begin{aligned} \left| (F(\mathcal{T}) - \hat{F}(\mathcal{T})) - (F(\mathcal{T}') - \hat{F}(\mathcal{T}')) \right| &\leq L_\sigma \left(\mathbb{E}_{\mathbf{x}} U(\mathbf{x}) + \frac{1}{N} \sum_{n=1}^N U(\mathbf{x}_n) \right) \|\mathcal{T} - \mathcal{T}'\| \\ &\leq 2L_\sigma U_{\max} \|\mathcal{T} - \mathcal{T}'\|. \end{aligned}$$

By Proposition 5 of Cucker & Smale (2001), we can cover the ball $\{\mathcal{T} : \|\mathcal{T}\| \leq R\}$ with at most $(4R/\eta)^{Bd}$ balls of radius η with respect to the metric $\|\mathcal{T} - \mathcal{T}'\|$. So, to construct our covering argument, we apply the (bidirectional) Hoeffding inequality to the center of each of these balls, with failure probability $\delta/(4R/\eta)^{Bd}$ for each. Combining this with how much $F - \hat{F}$ can change between an arbitrary point in $\{\mathcal{T} : \|\mathcal{T}\| \leq R\}$ and the nearest center, we have that for all $\eta \in (0, R)$, it holds with probability at least $1 - \delta$ that

$$\sup_{\mathcal{T}} \left| F(\mathcal{T}) - \hat{F}(\mathcal{T}) \right| \leq 2L_\sigma U_{\max} \eta + U_{\max} \sqrt{\frac{Bd}{2N} \log \frac{4R}{\eta} + \frac{1}{2N} \log \frac{2}{\delta}}.$$

The result follows by picking $\eta = 4\sqrt{B/N}$ and using $\log(a) = \frac{1}{2} \log(a^2)$. \square

A.2 PARAMETER ADAPTATION

Proposition 3. *If $\forall \mathbf{x} \in \mathcal{U}, U(\mathbf{x}; f) \rightarrow c$ where $c \geq 0$, the estimated UCoverage $\widehat{UC}_{k_\sigma}(\mathcal{S})$ approaches the estimated GCoverage $\widehat{C}_{k_\sigma}(\mathcal{S})$, up to a constant.*

Proof. As $U(\mathbf{x}) \rightarrow c \forall \mathbf{x} \in \mathcal{X}$, the following equality holds:

$$\begin{aligned} \lim_{U(\mathbf{x}) \rightarrow c} \widehat{UC}_{k_\sigma}(\mathcal{S}) &= \lim_{U(\mathbf{x}) \rightarrow c} \frac{1}{N} \sum_{n=1}^N U(\mathbf{x}_n) \cdot \max_{\mathbf{x}' \in \mathcal{S}} k_\sigma(\mathbf{x}_n, \mathbf{x}') \\ &= \frac{1}{N} \sum_{n=1}^N \lim_{U(\mathbf{x}_n) \rightarrow c} U(\mathbf{x}_n) \cdot \max_{\mathbf{x}' \in \mathcal{S}} k_\sigma(\mathbf{x}_n, \mathbf{x}') = c \cdot \widehat{C}_{k_\sigma}(\mathcal{S}). \end{aligned}$$

The last equality holds since each term with limit inside the sum converges to a specific value. \square

Proposition 4. *Suppose $k_\sigma(\mathbf{x}, \mathbf{x}'; g) = \psi((g(\mathbf{x}) - g(\mathbf{x}')/\sigma)$ for a fixed $g : \mathcal{X} \rightarrow \mathbb{R}^d$ which is injective on \mathcal{U} , and a function $\psi : \mathbb{R}^d \rightarrow [0, 1]$ with $\psi(0) = 1$ and for all $t \in \mathbb{R}^d$ with $\|t\| = 1$, $\lim_{a \rightarrow \infty} \psi(at) = 0$. If $\sigma \rightarrow 0$, the estimated uncertainty coverage $\widehat{UC}_{k_\sigma}(\mathcal{S})$ approaches $\sum_{s=1}^{|\mathcal{S}|} U(\mathbf{x}_s; f)$, up to a constant.*

Proof. As $\sigma \rightarrow 0$, the function k_σ approaches to the following form:

$$k_\sigma(\mathbf{x}, \mathbf{x}') = \begin{cases} 1 & \text{if } \mathbf{x} = \mathbf{x}', \\ 0 & \text{otherwise.} \end{cases}$$

Then, we have

$$\begin{aligned} \widehat{UC}_{k_\sigma}(\mathcal{S}) &= \frac{1}{N} \sum_{n=1}^N U(\mathbf{x}_n) \cdot \max_{\mathbf{x}' \in \mathcal{S}} k_\sigma(\mathbf{x}_n, \mathbf{x}') \\ &= \frac{1}{N} \sum_{n=1}^N U(\mathbf{x}_n) \cdot \mathbb{1}[\exists \mathbf{x}' \in \mathcal{S} \text{ s.t. } \mathbf{x}_n = \mathbf{x}'] \propto \sum_{s=1}^{|\mathcal{S}|} U(\mathbf{x}_s) \end{aligned}$$

Note that the indicator function is 1 only if \mathbf{x}_n is equal to one of data points in \mathcal{S} . \square

A.3 GREEDY ALGORITHM

Corollary 6. *In the setting of Theorem 2, let $\hat{\mathcal{S}} \subseteq \mathcal{U}$ be the result of UHerding for B steps to add to \mathcal{L} , and $UC^* = \max_{\mathcal{S} \subseteq \mathcal{U}, |\mathcal{S}|=B} UC_{k_\sigma}(\mathcal{L} \cup \mathcal{S})$ the optimal coverage obtainable among \mathcal{U} . Then*

$$UC_{k_\sigma}(\mathcal{L} \cup \hat{\mathcal{S}}) \geq \left(1 - \frac{1}{e}\right) UC^* - \left(2 - \frac{1}{e}\right) U_{\max} \sqrt{\frac{B}{N}} \left[8L_\sigma + \frac{1}{2} \sqrt{d \log \left(R^2 \frac{N}{B} \right) + \frac{2}{B} \log \frac{2}{\delta}} \right].$$

Proof. First, \widehat{UC}_{k_σ} is submodular by Lemma 10. Thus, if we let $\bar{\mathcal{S}} \in \arg \max_{\mathcal{S} \subseteq \mathcal{U}: |\mathcal{S}|=B} \widehat{UC}_{k_\sigma}(\mathcal{S})$, the classical result of Nemhauser et al. (1978) implies that $\widehat{UC}_{k_\sigma}(\hat{\mathcal{S}}) \geq (1 - \frac{1}{e}) \widehat{UC}_{k_\sigma}(\bar{\mathcal{S}})$.

Let $\mathcal{S}^* \in \arg \max_{\mathcal{S} \subseteq \mathcal{U}: |\mathcal{S}|=B} UC_{k_\sigma}(\mathcal{S})$ be the optimal size- B subset of \mathcal{U} for UC_{k_σ} . By definition, $\widehat{UC}_{k_\sigma}(\bar{\mathcal{S}}) \geq \widehat{UC}_{k_\sigma}(\mathcal{S}^*)$. Thus, calling the bound on the worst-case absolute error of the coverage estimate ε , it holds with probability at least $1 - \delta$ that

$$UC_{k_\sigma}(\hat{\mathcal{S}}) \geq \widehat{UC}_{k_\sigma}(\hat{\mathcal{S}}) - \varepsilon \geq \left(1 - \frac{1}{e}\right) \widehat{UC}_{k_\sigma}(\mathcal{S}^*) - \varepsilon \geq \left(1 - \frac{1}{e}\right) UC_{k_\sigma}(\mathcal{S}^*) - \left(2 - \frac{1}{e}\right) \varepsilon. \quad \square$$

The following result guarantees that greedy optimization of UC_{k_σ} or \widehat{UC}_{k_σ} achieves a $(1 - 1/e)$ approximation, by the result of Nemhauser et al. (1978).

Lemma 10. *The functions UC_{k_σ} and $\widehat{\text{UC}}_{k_\sigma}$ are nonnegative, submodular, monotone functions; thus so are the functions $\mathcal{S} \mapsto \text{UC}_{k_\sigma}(\mathcal{L} \cup \mathcal{S})$ and $\mathcal{S} \mapsto \widehat{\text{UC}}_{k_\sigma}(\mathcal{L} \cup \mathcal{S})$ for any fixed \mathcal{L} .*

Proof. We prove that UCoverage is non-negative monotone submodular; this implies that $\widehat{\text{UC}}_{k_\sigma}$ is as well, as it is an instance of UC_{k_σ} with an empirical distribution for \mathbf{x} .

For $\mathbf{x}, \mathbf{x}' \in \mathcal{X}$, we assumed that $U(\mathbf{x}) \geq 0$ and $k_\sigma(\mathbf{x}, \mathbf{x}') \geq 0$. Thus, for any subset $\mathcal{A} \subseteq \mathcal{X}$, $\text{UC}_{k_\sigma}(\mathcal{A}) \geq 0$.

Next, we show monotonicity: for all $\mathcal{A} \subseteq \mathcal{B} \subseteq \mathcal{X}$, $\text{UC}_{k_\sigma}(\mathcal{A}) \leq \text{UC}_{k_\sigma}(\mathcal{B})$.

$$\begin{aligned} \text{UC}_{k_\sigma}(\mathcal{B}) &= \mathbb{E}_{\mathbf{x}}[U(\mathbf{x}) \cdot \max_{\mathbf{x}' \in \mathcal{B}} k_\sigma(\mathbf{x}, \mathbf{x}')] \\ &= \mathbb{E}_{\mathbf{x}} \left[U(\mathbf{x}) \cdot \max \left(\max_{\mathbf{x}' \in \mathcal{B} \setminus \mathcal{A}} k_\sigma(\mathbf{x}, \mathbf{x}'), \max_{\mathbf{x}' \in \mathcal{A}} k_\sigma(\mathbf{x}, \mathbf{x}') \right) \right] \\ &\geq \mathbb{E}_{\mathbf{x}}[U(\mathbf{x}) \cdot \max_{\mathbf{x}' \in \mathcal{A}} k_\sigma(\mathbf{x}, \mathbf{x}')] = \text{UC}_{k_\sigma}(\mathcal{A}). \end{aligned}$$

Lastly, we show submodularity: for all $\mathcal{A} \subseteq \mathcal{B} \subseteq \mathcal{X}$,

$$\begin{aligned} \text{UC}_{k_\sigma}(\mathcal{A} \cup \{\tilde{\mathbf{x}}\}) - \text{UC}_{k_\sigma}(\mathcal{A}) &= \mathbb{E}_{\mathbf{x}} \left[U(\mathbf{x}) \cdot \max \left(k_\sigma(\mathbf{x}, \tilde{\mathbf{x}}) - \max_{\mathbf{x}' \in \mathcal{A}} k_\sigma(\mathbf{x}, \mathbf{x}'), 0 \right) \right] \\ &\geq \mathbb{E}_{\mathbf{x}} \left[U(\mathbf{x}) \cdot \max \left(k_\sigma(\mathbf{x}, \tilde{\mathbf{x}}) - \max_{\mathbf{x}' \in \mathcal{B}} k_\sigma(\mathbf{x}, \mathbf{x}'), 0 \right) \right] \\ &= \text{UC}_{k_\sigma}(\mathcal{B} \cup \{\tilde{\mathbf{x}}\}) - \text{UC}_{k_\sigma}(\mathcal{B}). \quad \square \end{aligned}$$

A.4 CONNECTIONS TO HYBRID METHODS

Proposition 7 (Weighted k -means of Zhdanov 2019). *Define an uncertainty measure $U(\mathbf{x}; f)$ from another uncertainty measure $U'(\mathbf{x}; f)$ as $U(\mathbf{x}; f) := U'(\mathbf{x}; f) \cdot \mathbb{1}[U'(\tilde{\mathbf{x}}; f) \geq \nu]$, where $\nu \geq 0$ satisfies $\sum_{n=1}^N \mathbb{1}[U'(\mathbf{x}_n; f) \geq \nu] = M$, a pre-defined number. Then weighted k -means with uncertainty U' , changed to use greedy kernel k -medoids, is UHerding with uncertainty U and the same kernel.*

Proof. With the modification of the k -means objective into a greedy kernel k -medoids objective, the objective of weighted k -means with $U'(\mathbf{x})$ as weights can be converted into:

$$\mathbf{x}^* \in \arg \max_{\tilde{\mathbf{x}} \in \mathcal{X}} \mathbb{1}[U'(\tilde{\mathbf{x}}) \geq \nu] \cdot \frac{1}{N} \sum_{n=1}^N U'(\mathbf{x}_n) \cdot \min_{x' \in \mathcal{L} \cup \{\tilde{\mathbf{x}}\}} \|\phi(\mathbf{x}_n) - \phi(\mathbf{x}')\|_{\mathcal{H}}^2 \quad (5)$$

$$= \arg \max_{\tilde{\mathbf{x}} \in \mathcal{X}} \frac{1}{N} \sum_{n=1}^N U(\mathbf{x}_n) \cdot \min_{x' \in \mathcal{L} \cup \{\tilde{\mathbf{x}}\}} \|\phi(\mathbf{x}_n) - \phi(\mathbf{x}')\|_{\mathcal{H}}^2 \quad (6)$$

$$= \arg \max_{\tilde{\mathbf{x}} \in \mathcal{X}} \frac{1}{N} \sum_{n=1}^N U(\mathbf{x}_n) \cdot \max_{x' \in \mathcal{L} \cup \{\tilde{\mathbf{x}}\}} k_\sigma(\mathbf{x}_n, \mathbf{x}'). \quad (7)$$

This is equivalent to the objective of UHerding with $U(\mathbf{x})$ as the choice of uncertainty. \square

Proposition 8 (ALFA-Mix of Parvaneh et al. 2022). *Let $\hat{y}(\cdot; f)$ be the predicted label of an input under f . Define an uncertainty measure*

$$U(\mathbf{x}; f) := \mathbb{1}[\exists \text{ class } j \text{ s.t. } \hat{y}(\alpha_j(\mathbf{x})g(\mathbf{x}) + (1 - \alpha_j(\mathbf{x}))\bar{g}_j; f) \neq \hat{y}(g(\mathbf{x}); f)] \quad (3)$$

where \bar{g}^j is the mean of feature representations belonging to class j and $\alpha_j(\mathbf{x}) \in [0, 1]$ is the same parameter as determined by ALFA-Mix. Then ALFA-Mix, with clustering replaced by greedy kernel k -medoids, is UHerding with uncertainty U and the same kernel.

Proof. ALFA-Mix selects closest data points to the center of k -means clusters where k -means is fitted with filtered data points. It keeps a data point \mathbf{x} if it satisfies that $\exists \text{ class } j \text{ s.t. } \hat{y}(\alpha_j(\mathbf{x})g(\mathbf{x}) + (1 - \alpha_j(\mathbf{x}))\bar{g}_j; f) \neq \hat{y}(g(\mathbf{x}); f)$, which we can express as the indicator function in Equation (3).

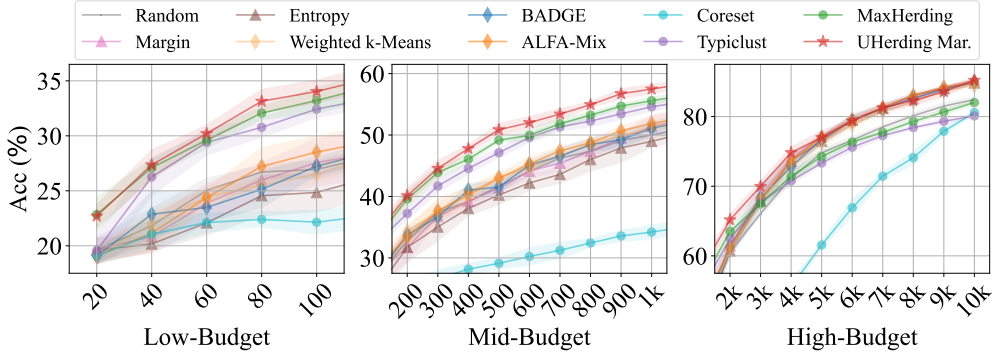


Figure 7: Comparison on CIFAR10 for supervised-learning tasks.

With the replacement of k -means with a greedy kernel k -medoids objective, the objective of ALFA-Mix can be converted into:

$$\mathbf{x}^* \in \arg \max_{\tilde{\mathbf{x}} \in \mathcal{X}} \frac{1}{N} \sum_{n=1}^N U(\mathbf{x}; f) \cdot \max_{\mathbf{x}' \in \mathcal{L} \cup \{\tilde{\mathbf{x}}\}} k_{\sigma}(\mathbf{x}_n, \mathbf{x}'). \quad \square$$

Proposition 9 (BADGE, Ash et al., 2020). *If $\forall \mathbf{x} \in \mathcal{U}$, $\hat{p}(\mathbf{x}; f) \rightarrow \frac{1}{K} \vec{1}$, then this BADGE approaches a slightly modified MaxHerding: $(\mathbb{1}[\hat{y}(\mathbf{x}_n; f) = \hat{y}(\mathbf{x}'; f)] - \frac{1}{K}) k_{\sigma}(\mathbf{x}_n, \mathbf{x}'; g)$ instead of $k_{\sigma}(\mathbf{x}_n, \mathbf{x}'; g)$. If $\sigma \rightarrow 0$, it approaches to the uncertainty-based method where uncertainty is defined as $U''(\tilde{\mathbf{x}}) := \min_{\mathbf{x}' \in \mathcal{L} \cup \{\tilde{\mathbf{x}}\}} \|\hat{y}(\mathbf{x}'; f) - \hat{p}(\mathbf{x}'; f)\|_2^2$.*

Proof. Recall $q(\mathbf{x}) = \hat{y}(\mathbf{x}; f) - \hat{p}(\mathbf{x}; f)$. As $\forall \mathbf{x} \in \mathcal{U}$, $\hat{p}(\mathbf{x}; f) \rightarrow \frac{1}{K} \vec{1}$, it is true that $\|q(\mathbf{x})\|_2^2 \rightarrow 1 - \frac{1}{K}$ and $\langle q(\mathbf{x}), q(\mathbf{x}') \rangle \rightarrow \mathbb{1}[\hat{y}(\mathbf{x}_n; f) = \hat{y}(\mathbf{x}'; f)] - \frac{1}{K}$. With the assumption that $\forall \mathbf{x} \in \mathcal{X}$, $k_{\sigma}(\mathbf{x}, \mathbf{x}; g) = c$,

$$h(\mathbf{x}_n, \mathbf{x}') \rightarrow 2 \left(\mathbb{1}[\hat{y}(\mathbf{x}_n; f) = \hat{y}(\mathbf{x}'; f)] - \frac{1}{K} \right) k_{\sigma}(\mathbf{x}_n, \mathbf{x}'; g) - 2c \left(1 - \frac{1}{K} \right). \quad (8)$$

Therefore, the following is true:

$$\mathbf{x}^* \in \arg \max_{\tilde{\mathbf{x}} \in \mathcal{U}} \frac{1}{N} \sum_{n=1}^N \max_{\mathbf{x}' \in \mathcal{L} \cup \{\tilde{\mathbf{x}}\}} h(\mathbf{x}_n, \mathbf{x}') \quad (9)$$

$$= \arg \max_{\tilde{\mathbf{x}} \in \mathcal{U}} \frac{1}{N} \sum_{n=1}^N \max_{\mathbf{x}' \in \mathcal{L} \cup \{\tilde{\mathbf{x}}\}} \left(\mathbb{1}[\hat{y}(\mathbf{x}_n; f) = \hat{y}(\mathbf{x}'; f)] - \frac{1}{K} \right) k_{\sigma}(\mathbf{x}_n, \mathbf{x}'; g). \quad (10)$$

If $\sigma \rightarrow 0$, $k_{\sigma}(\mathbf{x}, \mathbf{x}'; g) = \mathbb{1}[\mathbf{x} = \mathbf{x}']$. Then, $\max_{\mathbf{x}' \in \mathcal{L} \cup \{\tilde{\mathbf{x}}\}} h(\mathbf{x}_n, \mathbf{x}') \rightarrow \min_{\mathbf{x}' \in \mathcal{L} \cup \{\tilde{\mathbf{x}}\}} \|q(\mathbf{x}_n)\|_2^2 + \|q(\mathbf{x}')\|_2^2 = \min_{\mathbf{x}' \in \mathcal{L} \cup \{\tilde{\mathbf{x}}\}} \|\hat{y}(\mathbf{x}'; f) - \hat{p}(\mathbf{x}'; f)\|_2^2$. Then,

$$\mathbf{x}^* \in \arg \max_{\tilde{\mathbf{x}} \in \mathcal{U}} \frac{1}{N} \sum_{n=1}^N \max_{\mathbf{x}' \in \mathcal{L} \cup \{\tilde{\mathbf{x}}\}} h(\mathbf{x}_n, \mathbf{x}') \quad (11)$$

$$= \arg \max_{\tilde{\mathbf{x}} \in \mathcal{U}} \min_{\mathbf{x}' \in \mathcal{L} \cup \{\tilde{\mathbf{x}}\}} \|\hat{y}(\mathbf{x}'; f) - \hat{p}(\mathbf{x}'; f)\|_2^2 \quad (12)$$

Therefore, BADGE approaches to $\arg \max_{\tilde{\mathbf{x}} \in \mathcal{U}} U''(\tilde{\mathbf{x}})$ as $\sigma \rightarrow 0$. \square

B ADDITIONAL COMPARISON WITH STATE OF THE ART

In addition to Figure 4 where we compare state-of-the-art active learning methods on CIFAR100 and TinyImageNet datasets for supervised learning tasks, we provide Figure 7 for additional results on CIFAR10 dataset. Again, we employ a ResNet18 randomly initialized at each iteration.

Similar to the results on CIFAR100 and TinyImageNet datasets, UHerdg significantly outperforms representation-based methods in high-budget regimes, and uncertainty-based methods in low- and mid-budget regimes, confirming the robustness of UHerdg over other active learning methods.

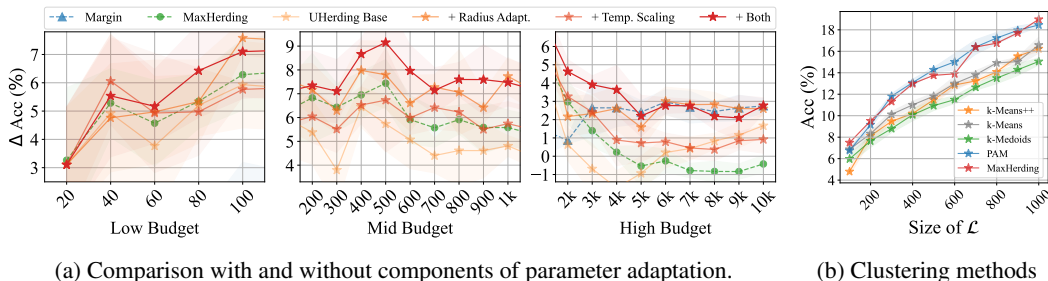


Figure 8: Comparison of some components in UHerding (Left) and clustering methods (Right)

C COMPONENT ANALYSIS OF UHERDING

In this ablation study, we examine the contribution of each component of UHerding to its overall generalization performance. Specifically, we incrementally add each of temperature scaling (Temp. Scaling) and adaptive radius (Radius Adap.) individually to the UHerding baseline, which selects data points based solely on the UHerding acquisition defined in Equation (2). We also evaluate the combined effect of both components. As in Section 4.1, we use CIFAR-10 dataset, and present the results using ΔAcc relative to Random selection to clearly highlight the differences.

Although temperature scaling enhances performance over the UHerding baseline, its performance is still comparable to MaxHerding in the low-budget regime, and worse than Margin in the high-budget regime. Radius adaptation generally matches or exceeds MaxHerding across budget regimes but quickly converges to Margin’s performance in the high-budget regime. When both temperature scaling and radius adaptation are applied, performance surpasses both MaxHerding and Margin across all budget regimes, with saturation in the high-budget regime occurring significantly more gradually than with radius adaptation alone. Please note that Margin’s performance in the low- and mid-budget regimes is not visible due to its exceptionally poor results relative to other methods.

D COMPARISON OF CLUSTERING METHODS

As noted in Section 2, we compare several clustering methods applied to BADGE Ash et al. (2020) to justify the replacement of k -means and k -means++ of existing active learning methods with MaxHerding. Figure 8b compares k -means, k -means++, k -medoids (iterative optimization), partition around medoids (PAM), and MaxHerding, a greedy kernel k -medoids. We train a ResNet18 randomly initialized at each iteration on CIFAR100.

Surprisingly, k -medoids performs slightly worse than k -means, showing that searching for medoids is not necessarily better than search of means. However, the gap between PAM and k -medoids shows that optimization methods do make significant changes. Although PAM works the best overall, MaxHerding is comparable with much less computation Bae et al. (2024). It justifies the replacement of k -means and k -means++ with MaxHerding for existing active learning methods.